A New Decorrelating RAKE Receiver for Long-code WCDMA

L. Tong[1]
Dept of Elec. & Comp. Engr.
Cornell University
Ithaca, NY 14850
ltong@ece.cornell.edu

A. van der Veen and P. Dewilde
Department of Elec. Engr.
Delft University of Technology
Delft, The Netherlands
{allejan,dewilde}@cas.et.tudelft.nl

Abstract — **A RAKE receiver using a decorrelating matched filter is proposed for the joint channel and symbol estimation for long-code wideband CDMA. Channel parameters and data symbols are estimated jointly by least squares via rank-one decompositions. An identifiability condition is established, which suggests that channels unidentifiable in short code CDMA systems are almost surely identifiable when aperiodic spreading codes are used. An efficient implementation of the decorrelating matched filter is proposed based on time-varying state space realizations, which makes the complexity of the proposed decorrelating RAKE comparable with that of the conventional RAKE receiver. The mean square error of the estimated channel is compared to the Cramér-Rao bound.**

I. Introduction

We consider the problem of joint channel estimation and symbol detection in a long-code wideband CDMA system that has features of third generation wireless standards such as UMTS. The scrambling sequences of users are aperiodic; data and control information may be modulated onto the in-phase and quadrature parts of the signal using different channelization codes. Pilots may be part of the control symbols. To support multimedia applications, users may have different spreading gains, or multiple channelization codes may be assigned to the same user. Users are asynchronous, and their multipath channels may have delay spread longer than the symbol period. Multiple antennas may be used.

The RAKE structure is widely used in CDMA. For high rate CDMA under frequency selective fading, however, code orthogonality can not be guaranteed, and the conventional RAKE receiver that uses a bank of matched filters may perform poorly. The loss of code orthogonality has adverse effects on both channel estimation and symbol detection, and the performance degradation is especially pronounced when the network is heavily loaded and power control imperfect.

In this paper, we propose a channel estimation and symbol detection scheme for RAKE receivers. As illustrated in Fig. 1, a decorrelating matched filter projects the received chip-rate signal $y[n]$ into the signal space of each user. Channel coefficients and the symbol sequence of each user can then be estimated, jointly and independent of other users, by least squares via rank one decompositions. This algorithm imposes no conditions on channel parameters and is capable of dealing with rapid multipath fading. We also establish a new identifiability condition that depends only on the spreading codes used in the system but not on channel parameters. Implied by this identifiability condition is that the use of long codes enhances channel identifiability; channels not identifiable in short-code CDMA are almost surely identifiable in a long code system.

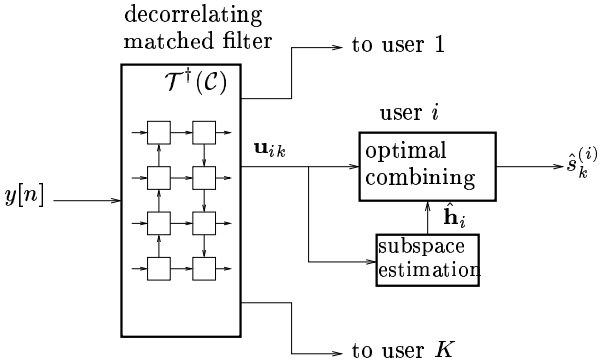

Figure 1: Receiver structure. The decorrelating matched filter is implemented by an efficient state-space realization.

A key contribution of this work is an efficient implementation of the decorrelating matched filter. The idea of using the decorrelating matched filter for short code CDMA is known [1], but applying it to long code CDMA using current technology presents a daunting task. Fortunately, there is an extensive theory and algorithms developed by Dewilde and Van der Veen [2] who considered the inversion of infinite size structured matrices. Their approach leads to a state-space implementation of the the decorrelating receiver at the same level of complexity as that of the conventional matched filter.

Related Work Blind channel estimation and multiuser detection for long code CDMA has been considered by a number of other authors. Iterative techniques based on maximizing the likelihood function [3, 4] and least squares [5] have been proposed. These are high perfor-

[1]The research of Lang Tong was partially carried out as part of a visiting professorship granted by the Cor Wit Foundation. This work was also supported in part by the Multidisciplinary University Research Initiative (MURI) under the Office of Naval Research Contract N00014-00-1-0564

mance techniques but also have well known drawbacks such as ill convergence and high complexity. They are best complemented by good initialization techniques such as the algorithm developed in this paper. Also in the literature are second order moment techniques based on the i.i.d. assumption of the spreading code or the symbols [6–9]. These techniques rely on the convergence of time averages to statistical averages, which often requires hundreds to thousands of symbols. The work of Weiss and Friedlander [10] is perhaps the closest to our approach although they focus on down link applications. They assume that multipath delays are limited to a small fraction of a symbol interval. By dropping samples that contain intersymbol interference, they propose to invert the code matrix followed by a different subspace algorithm and an iterative likelihood maximization. Their assumptions imply that their algorithm is not applicable to systems with asynchronous users and long multipath delays.

II. Data Model

Several derivations of data models for long code CDMA exist [10,11], all lead to the similar matrix equation used in this paper. Here we present the model graphically to avoid unnecessary cluttering of notations. An algebraic derivation of the model based on Nyquist sampling is given in [12]. That model also applies to multiple receiving antennas. Results presented here only need minor and obvious modifications.

We assume that the transmissions are slotted, and each user transmits M_i symbols. Data for the entire slot are collected for processing. Because the channel is linear, we first focus on symbol s_{ik} from user i transmitted in the kth symbol interval, assuming all other symbols and noise are zero. Let the received signal corresponding to symbol s_{ik} be passed through a chip-matched filter and sampled at the chip rate. All samples are put in a vector $\mathbf{y}_{ik}$. As shown in Fig 2, $\mathbf{y}_{ik}$ is made of a linear combination of shifted (delayed) code vectors $\mathbf{c}_{ik}$ which is the segment of the spreading code of user i corresponding to the kth symbol. Each shifted code vector is multiplied by the jth fading coefficient h_{ij}, and the channel response to s_{ik} is given by

$$\mathbf{y}_{ik} = \mathcal{T}_k(\mathcal{C}_i)\mathbf{h}_i s_{ik}, \tag{1}$$

where $\mathcal{T}_k(\mathcal{C}_i)$ is the code matrix of user i and symbol k (See Fig 2(a)), and $\mathbf{h}_i$ is the multipath fading channel for user i. One can view that each column of $\mathcal{T}_k(\mathcal{C}_i)$ corresponds to a discrete multipath. For example, the first column of $\mathcal{T}_k(\mathcal{C}_i)$ is made of $(k-1)G_i + D_i$ zeros that model the relative delay of the first path with respect to the reference followed by the code vector $\mathbf{c}_{ik}$ and additional zeros that make the size of $\mathbf{y}_{ik}$ the total number of chips of the entire frame. The second column of $\mathcal{T}_k(\mathcal{C}_i)$ models the second multipath similarly. Note that for sparse channels, the shifting of the code vectors does not have to be consecutive.

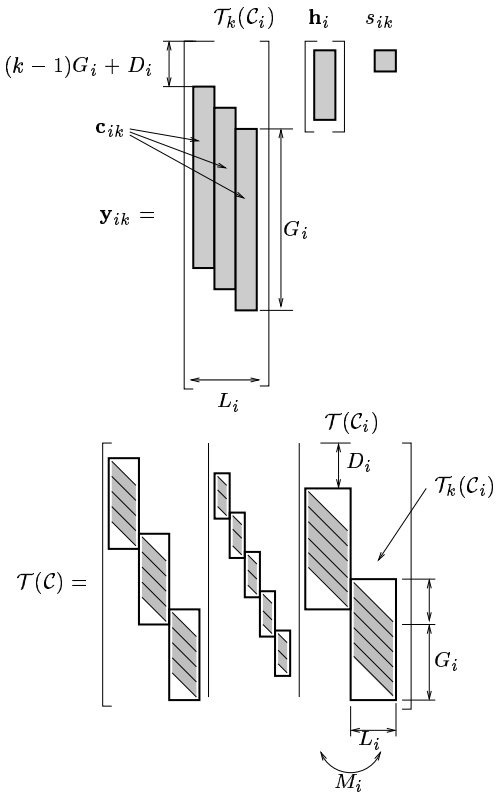

Figure 2: (a) Structure of $\mathcal{T}_k(\mathcal{C}_i)$; (b) Structure of the code matrix $\mathbf{T}$.

For user i, the total received noiseless signal is given by

$$\mathbf{y}_i = \sum_{k=1}^{M_i} \mathcal{T}_k(\mathcal{C}_i)\mathbf{h}_i s_{ik} = \mathcal{T}(\mathcal{C}_i)(\mathbf{I}_{M_i} \otimes \mathbf{h}_i)\mathbf{s}_i, \tag{2}$$

where $\mathbf{s}_i$ contains all symbols from user i, and

$$\mathcal{T}(\mathcal{C}_i) \triangleq [\mathcal{T}_1(\mathcal{C}_i), \cdots, \mathcal{T}_{M_i}(\mathcal{C}_i)] \tag{3}$$

is the code matrix of user i, and it has a special block shifting structure. Specifically, $\mathcal{T}_m(\mathcal{C}_i)$ is the shift of $\mathcal{T}_{m-1}(\mathcal{C}_i)$ by G_i positions. This structure will be exploited in Sec. IV.

Including all users, again referring to Fig 2, we have the complete matrix model

$$\mathbf{y} = \mathcal{T}(\mathcal{C})\mathcal{D}(\mathbf{h})\mathbf{s} + \mathbf{w}, \tag{4}$$

$$\mathcal{T}(\mathcal{C}) \triangleq [\mathcal{T}(\mathcal{C}_1)\cdots\mathcal{T}(\mathcal{C}_K)], \tag{5}$$

$$\mathcal{D}(\mathbf{h}) \triangleq diag(\mathbf{I}_{M_1} \otimes \mathbf{h}_1, \cdots, \mathbf{I}_{M_K} \otimes \mathbf{h}_K). \tag{6}$$

Note that, by allowing the code matrices $\mathcal{T}(\mathcal{C}_i)$ for each users having different sizes, we include cases when different spreading gains are used.

We will impose the following assumptions.

(A1): The code matrix $\mathcal{T}(\mathcal{C})$ is known.

(A2): The code matrix $\mathcal{T}(\mathcal{C})$ has full column rank.

(A3): The noise vector is complex Gaussian $\mathbf{w} \sim \mathcal{N}(\mathbf{0}, \sigma^2\mathbf{I})$ with possibly unknown σ^2.

Assumption (A1) implies that the receiver knows the codes, the delay offsets D_i, and the number of channel coefficients L_i of all users. If D_i is unknown, we may set it to 0 and model all paths. L_i is a modeling parameter and its choice is often left to algorithm designers. Since channel coefficients may be zero, one can over-parameterize the channel to accommodate channel length and delay uncertainties. Sometimes, the channel is sparse, and it is more efficient to model the channel as separate clusters of fingers. In that case, we assume that the approximate locations of these clusters are known.

Assumption (A2) is sufficient but not necessary for the channel to be identifiable and for the proposed algorithm to produce good estimates. This condition can of course be verified off line and is easy to satisfy for relatively large spreading gains. When (A2) fails, the channel may still be identifiable, and the proposed identification algorithm can be applied with simple modifications. See [13].

III. Blind and Semiblind Decorrelating RAKE

We present in this section the decorrelating RAKE Receiver that jointly estimates channel $\mathbf{h}$ and data $\mathbf{s}$. As illustrated in Fig. 1, the decorrelating RAKE is different from the conventional RAKE in that a decorrelating matched filter $\mathcal{T}^\dagger(\mathcal{C})$ is used to remove all multiaccess interference. We will present the details of an efficient time-varying state-space implementation of the decorrelating matched filter in Sec. IV. We note here only that the complexity of the decorrelating RAKE is comparable with that of the conventional one.

The output of the decorrelating matched filter is given by

$$\mathbf{u} = \mathcal{T}^\dagger(\mathcal{C})\mathbf{y} = diag(\mathbf{I}\otimes\mathbf{h}_1, \cdots, \mathbf{I}\otimes\mathbf{h}_K)\mathbf{s} + \mathbf{n}, \qquad (7)$$

where $\mathbf{n} = \mathcal{T}^\dagger(\mathcal{C})\mathbf{w}$ is now colored. Partition $\mathbf{u}$ into segments of length L_i with $\mathbf{u}_{ik}$ as the $(\sum_{j=1}^{i-1} M_j) + k$th subvector of $\mathbf{u}$. The structure of $\mathbf{u}$ in (7) implies that $\mathbf{u}_{ik}$ corresponds to symbol k of user i,

$$\mathbf{u}_{ik} = \mathbf{h}_i s_{ik} + \mathbf{n}_{ik}, \quad k = 1, \cdots, M_i\,, \qquad (8)$$

and is free from multi-user interference. Collecting all data for user i gives

$$\mathbf{U}_i = [\mathbf{u}_{i1}, \cdots, \mathbf{u}_{iM_i}] = \mathbf{h}_i\mathbf{s}_i^T + \mathbf{N}_i\,. \qquad (9)$$

Treating $\mathbf{h}_i$ and $\mathbf{s}_i$ as deterministic parameters, the least squares estimator of the outer product $\mathbf{h}_i\mathbf{s}_i^T$ is given by

$$\min_{\mathbf{h},\mathbf{s}_i} \| \mathbf{U}_i - \mathbf{h}_i\mathbf{s}_i^T \|_F^2$$

which produces estimates of $\mathbf{h}_i$ and $\mathbf{s}_i$ (with an unknown scaling factor) from a rank-one approximation of $\mathbf{U}_i$. In other words, denoting

$$\hat{\mathbf{R}}_i \triangleq \frac{1}{M_i}\sum_{k=1}^{M_i} \mathbf{u}_{ik}\mathbf{u}_{ik}^H\,, \qquad (10)$$

we obtain the least squares estimator

$$\hat{\mathbf{h}}_i = \arg\max_{\|\mathbf{g}\|=1} \mathbf{g}^H\hat{\mathbf{R}}_i\mathbf{g}\,, \quad \hat{s}_{ik} = \hat{\mathbf{h}}_i^H\mathbf{u}_{ik}\,. \qquad (11)$$

The solution $\hat{\mathbf{h}}_i$ is given as the dominant eigenvector of $\hat{\mathbf{R}}_i$. The scaling ambiguity in the above estimate must be removed by either incorporating prior knowledge of the symbol, using pilot symbols, or employing differential encoding of s_{ik}.

If arbitrarily placed pilot symbols exist in $\mathbf{s}_i$, the above least squares problem can be amended. Let $\mathbf{s}_i$ be partitioned into two subvectors, $\mathbf{s}_{i_p}$ contains the pilot and $\mathbf{s}_{i_d}$ the data. We partition $\mathbf{U}_i$ accordingly to $\mathbf{U}_{i_p}$ and $\mathbf{U}_{i_d}$. The least squares estimator is given by

$$\hat{\mathbf{h}}_i = \arg\min_{\mathbf{h},\mathbf{s}}\{\| \mathbf{U}_{i_p} - \mathbf{h}\mathbf{s}_{ip}^T \|_F^2 + \| \mathbf{U}_{i_d} - \mathbf{h}\mathbf{s}^T \|_F^2\}. \qquad (12)$$

The above optimization does not have a closed-form solution. Simple iterative schemes can be applied in lieu of (11. .

We now present an identifiability result that is more general than existing conditions. The condition is independent of the channel parameters, and can be checked easily off-line, and appropriate measures can be taken if it is not satisfied. More significant, perhaps, is that it decouples the identifiability of a particular user from that of others; one user's channel may be identifiable even when those of others are not. The proof of the following theorem gives the algorithm that identifies the channel when the identifiability condition holds.

Theorem 1 *Let $\mathcal{T}_k(\mathcal{C}_i)$ be the code matrix of user i for symbol k, and $\check{\mathcal{T}}_k(\mathcal{C}_i)$ the submatrix of $\mathcal{T}(\mathcal{C})$ after removing $\mathcal{T}_k(\mathcal{C}_i)$. The channel $\mathbf{h}_i$ of user i is identifiable if there exists a k such that*

$$\mathcal{R}\{\mathcal{T}_k(\mathcal{C}_i)\} \bigcap \mathcal{R}\{\check{\mathcal{T}}_k(\mathcal{C}_i)\} = \{\mathbf{0}\}. \qquad (13)$$

Because (13) only needs to hold for some k, the use of long codes in CDMA makes the identifiability condition easier to satisfy. For randomly generated codes, and large data size M, the channel is identifiable almost surely.

IV. Decorrelating Matched Filter

We now tackle the problem of inverting the code matrix $\mathcal{T}(\mathcal{C})$. Without an efficient technique to compute and apply the left inverse $\mathcal{T}^\dagger(\mathcal{C}) = [\mathcal{T}^H(\mathcal{C})\mathcal{T}(\mathcal{C})]^{-1}\mathcal{T}^H(\mathcal{C})$, the proposed receiver structure would not be feasible.

To simplify notation, we denote $\mathbf{T} \triangleq \mathcal{T}(\mathcal{C})$ which maps $\mathbf{u} \triangleq \mathcal{D}(\mathbf{h})\mathbf{s}$ to $\mathbf{y}$.

Consider an input signal $\mathbf{u}$ and output signal $\mathbf{y}$, with arbitrary block-partitioning

$$\mathbf{u} = \begin{bmatrix} \mathbf{u}_1 \\ \vdots \\ \mathbf{u}_N \end{bmatrix}, \qquad \mathbf{y} = \begin{bmatrix} \mathbf{y}_1 \\ \vdots \\ \mathbf{y}_N \end{bmatrix}.$$

The partitioning introduces the notion of "time", or a stage in a computational procedure. The blocks do not need to be of equal size, and some can even be empty-dimensional: this represents the absence of the corresponding input or output at that point in time.

A time-varying state space realization has the form

$$\begin{bmatrix} \mathbf{x}_{n+1} \\ \mathbf{y}_n \end{bmatrix} = \mathbf{T}_n \begin{bmatrix} \mathbf{x}_n \\ \mathbf{u}_n \end{bmatrix}, \qquad \mathbf{T}_n = \begin{bmatrix} \mathbf{A}_n & \mathbf{B}_n \\ \mathbf{C}_n & \mathbf{D}_n \end{bmatrix} \tag{14}$$

where $\mathbf{x}_n$ is a state vector which carries information from one stage of the computation to the next. A graphical representation of this is shown in Fig. 3. The state space realization specifies a mapping of $\mathbf{u}$ to $\mathbf{y}$ which is necessarily causal; $\mathbf{y}_n$ does not depend on $\mathbf{u}_{n+1}$.

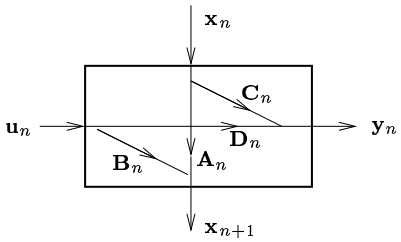

Figure 3: Time varying state space representation at time instant n.

Using the notion of zero dimensional vectors and matrices, we assume that the realization starts at time 1 with $\mathbf{x}_1 = \bullet$ (or no state), and ends at time N again with state $\mathbf{x}_{N+1} = \bullet$. Hence $\mathbf{A}_1 = \bullet$, $\mathbf{A}_N = \bullet$, $\mathbf{C}_1 = \bullet$, $\mathbf{B}_N = \bullet$.

Consider first an arbitrary $N \times L$ matrix matrix $\mathbf{T}$ with rows $\mathbf{t}_n^H$. A (trivial) state space realization that models $\mathbf{y} = \mathbf{T}\mathbf{u}$ is obtained by setting $\mathbf{u}_1 = \mathbf{u}$, $\mathbf{u}_2 = \cdots = \mathbf{u}_N = \bullet$ (i.e., the complete input vector is entered at time 1), and

$$\begin{bmatrix} \mathbf{A}_1 & \mathbf{B}_1 \\ \mathbf{C}_1 & \mathbf{D}_1 \end{bmatrix} = \begin{bmatrix} \bullet & \mathbf{I} \\ \bullet & \mathbf{t}_1^H \end{bmatrix}, \begin{bmatrix} \mathbf{A}_N & \mathbf{B}_N \\ \mathbf{C}_N & \mathbf{D}_N \end{bmatrix} = \begin{bmatrix} \bullet & \bullet \\ \mathbf{t}_N^H & \bullet \end{bmatrix}$$
$$\begin{bmatrix} \mathbf{A}_n & \mathbf{B}_n \\ \mathbf{C}_n & \mathbf{D}_n \end{bmatrix} = \begin{bmatrix} \mathbf{I} & \bullet \\ \mathbf{t}_n^H & \bullet \end{bmatrix}, \quad n = 2, \cdots, N-1.$$

Now consider an arbitrary block-partitioned matrix $\mathbf{T} = [\mathbf{T}^{(1)} \quad \mathbf{T}^{(2)}]$ where $\mathbf{T}^{(1)}$ has realization $\{\mathbf{A}_n^{(1)}, \mathbf{B}_n^{(1)}, \mathbf{C}_n^{(1)}, \mathbf{D}_n^{(1)}\}$ and $\mathbf{T}^{(2)}$ has realization $\{\mathbf{A}_n^{(2)}, \mathbf{B}_n^{(2)}, \mathbf{C}_n^{(2)}, \mathbf{D}_n^{(2)}\}$. Then $\mathbf{T}$ has realization

$$\mathbf{T}_n = \left[\begin{array}{cc|cc} \mathbf{A}_n^{(1)} & 0 & \mathbf{B}_n^{(1)} & 0 \\ 0 & \mathbf{A}_n^{(2)} & 0 & \mathbf{B}_n^{(2)} \\ \hline \mathbf{C}_n^{(1)} & \mathbf{C}_n^{(2)} & \mathbf{D}_n^{(1)} & \mathbf{D}_n^{(2)} \end{array}\right].$$

The structure of the realization is shown in Fig. 4.

The code matrix $\mathbf{T}$ in our case has a shift structure as shown in Fig. 2. By combining the two examples, we can represent any code matrix $\mathbf{T}$, irrespective of the processing gains G_i, offsets D_i, channel lengths L_i and number of symbols M_i (these can be different for each user).

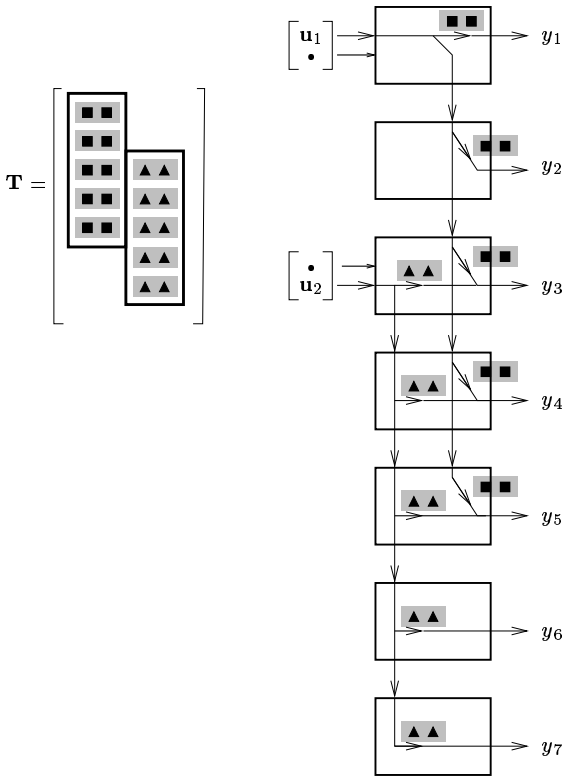

Figure 4: Computational network for block partitioned matrix.

The number of state space time points is equal to the number of rows of $\mathbf{T}$. Each state space stage has 1 (scalar) output. The input vector is partitioned in blocks of L_i entries which enter the system at appropriate time points, determined by the starting points of the individual code blocks. The state dimension at each time point is (usually) the number of nonzero entries in the corresponding row of $\mathbf{T}$ (less if the row contains the start or end of a block).

To compute the left inverse $\mathbf{T}^\dagger$, our aim is to first compute a QR factorization $\mathbf{T} = \mathbf{Q}\mathbf{R}$ where $\mathbf{Q}^{\mathrm{H}}\mathbf{Q} = \mathbf{I}$ and $\mathbf{R}$ is square and lower triangular, and then to invert each of the factors: $\mathbf{T}^\dagger = \mathbf{R}^{-1}\mathbf{Q}^{\mathrm{H}}$. The computation of the QR factorization can be done in state space, as is demonstrated by the following theorem.

Theorem 2 *Let* $\mathbf{T}$ *have a state space realization* $\{\mathbf{A}_n, \mathbf{B}_n, \mathbf{C}_n, \mathbf{D}_n\}_{n=1}^N$. *Assume that* $\mathbf{T}$ *has full column rank (*$\mathbf{T}^H\mathbf{T}$ *is full rank). Let* $\mathbf{Y}_{N+1} = \bullet$ *and consider the sequence of (economy-size) QR factorizations*

$$\begin{bmatrix} \mathbf{Y}_{n+1}\mathbf{A}_n & \mathbf{Y}_{n+1}\mathbf{B}_n \\ \mathbf{C}_n & \mathbf{D}_n \end{bmatrix} =: \underbrace{\begin{bmatrix} \mathbf{A}_n^Q & \mathbf{B}_n^Q \\ \mathbf{C}_n^Q & \mathbf{D}_n^Q \end{bmatrix}}_{\mathbf{Q}_n} \begin{bmatrix} \mathbf{Y}_n & 0 \\ \mathbf{C}_n^R & \mathbf{D}_n^R \end{bmatrix} \tag{15}$$

($n = N, N-1, \cdots, 1$*), where* $\mathbf{Q}_n$ *is isometric (*$\mathbf{Q}_n^{\mathrm{H}}\mathbf{Q}_n = \mathbf{I}$*), and the partitioning of the right factor is such that* $\mathbf{Y}_n$ *has the same number of columns as* $\mathbf{A}_n$, $\mathbf{D}_n^R$ *has the same*

number of columns as $\mathbf{D}_n$*, and both* $\mathbf{Y}_n$ *and* $\mathbf{D}_n^R$ *are full row rank. Then all* $\mathbf{D}_n^R$ *are square, lower triangular and invertible, and* $\mathbf{T} = \mathbf{QR}$ *where* $\mathbf{Q}$ *is isometric (*$\mathbf{Q}^H\mathbf{Q} = \mathbf{I}$*) and is given by the realization*

$$\mathbf{Q}_n = \begin{bmatrix} \mathbf{A}_n^Q & \mathbf{B}_n^Q \\ \mathbf{C}_n^Q & \mathbf{D}_n^Q \end{bmatrix},$$

and $\mathbf{R}$ *is lower triangular and invertible and given by the realization*

$$\mathbf{R}_n = \begin{bmatrix} \mathbf{A}_n & \mathbf{B}_n \\ \mathbf{C}_n^R & \mathbf{D}_n^R \end{bmatrix}.$$

Note that in our application, $\mathbf{A}_n$ and $\mathbf{B}_n$ are trivial, either identity matrices or zero dimensional. Hence the multiplication by $\mathbf{Y}_{n+1}$ is trivial and the only actual work in (15) is the QR factorization.

Theorem 3 *Suppose that* $\mathbf{R}$ *is a square invertible lower triangular matrix. Then its inverse is lower triangular too. If* $\mathbf{R}$ *has state space realization*

$$\mathbf{R}_n = \begin{bmatrix} \mathbf{A}_n^R & \mathbf{B}_n^R \\ \mathbf{C}_n^R & \mathbf{D}_n^R \end{bmatrix}, n = 1, \cdots, N$$

then $\mathbf{S} := \mathbf{R}^{-1}$ *has state space realization*

$$\mathbf{S}_n = \begin{bmatrix} \mathbf{A}_n^R - \mathbf{B}_n^R \mathbf{D}_n^{R^{-1}} \mathbf{C}_n^R & \mathbf{B}_n^R \mathbf{D}_n^{R^{-1}} \\ -\mathbf{D}_n^{R^{-1}} \mathbf{C}_n^R & \mathbf{D}_n^{R^{-1}} \end{bmatrix}, n = 1, \cdots, N$$

Theorem 4 *Suppose that* $\mathbf{Q}$ *is an isometry (*$\mathbf{Q}^H\mathbf{Q} = \mathbf{I}$*) with realization*

$$\mathbf{Q}_n = \begin{bmatrix} \mathbf{A}_n^Q & \mathbf{B}_n^Q \\ \mathbf{C}_n^Q & \mathbf{D}_n^Q \end{bmatrix}, \qquad n = 1, \cdots, N$$

where all $\mathbf{Q}_n$ *are isometric. Then* $\mathbf{Q}$ *has a left inverse* $\mathbf{Q}^H$ *with an* anticausal *state space realization*

$$\mathbf{Q}_n^H = \begin{bmatrix} \mathbf{A}_n^{Q^H} & \mathbf{C}_n^{Q^H} \\ \mathbf{B}_n^{Q^H} & \mathbf{D}_n^{Q^H} \end{bmatrix}, n = 1, \cdots, N \qquad (16)$$

The anti-causal realization in (16) corresponds to the equations (backward recursion)

$$\begin{cases} \mathbf{x}_n &= \mathbf{A}_n^{Q^H} \mathbf{x}_{n+1} + \mathbf{C}_n^{Q^H} \mathbf{u}_n \\ \mathbf{y}_n &= \mathbf{B}_n^{Q^H} \mathbf{x}_{n+1} + \mathbf{D}_n^{Q^H} \mathbf{u}_n \end{cases} \qquad n = N, N-1, \cdots, 1.$$

The state space realizations of $\mathbf{S}$ and $\mathbf{Q}^H$ are obtained *locally*, for every state matrix $\mathbf{R}_n$ and $\mathbf{Q}_n$ independently. Note that the preceding theorems can be used to invert more general matrices.

Complexity The complexity and storage requirement of $\mathbf{T}^\dagger$ in state-space factored form is about 2 times the number of non-zero entries in $\mathbf{T}$. This is only a factor 2 times the complexity of applying the matched filter $\mathbf{T}^H$. In contrast, note that $\mathbf{T}^\dagger = (\mathbf{T}^H\mathbf{T})^{-1}\mathbf{T}^H$ is a full matrix. The direct storage and multiplication complexity of a full $m \times n$ matrix is mn.

Thus, the benefit of the state-space approach in terms of complexity and storage is determined by the ratio of the number of non-zero entries over the total number of entries of $\mathbf{T}$. For our case, the number of nonzero entries (for users with equal parameters) is $MGLK$, whereas the total number of entries is M^2GLK. The benefit in complexity is thus in the order of M, the number of symbols per user per frame. See [13].

V. Simulation Results

In this section, we present some simulation results. For channel estimation, MSE is used and our estimator is compared with the CRB using Monte Carlo runs. For symbol detection, BER is used as the performance measure, and Monte Carlo runs are used to estimate the BER.

The Decorrelating RAKE receiver will be abbreviated as DRR and the conventional RAKE receiver RR.

The Simulation Setup Because our model is deterministic, simulations were conducted for a fixed channel and a fixed spreading code. When we evaluated the MSE of the channel estimator, the transmitted symbols were also fixed. In evaluating the BER, channels and spreading codes were fixed and the transmitted bits were generated randomly in each Monte Carlo run. The performance, of course varies with the channel and spreading parameters, but the qualitative behavior remains in our simulations. Specific parameters used in the simulation can be found in [12].

We considered a case with two asynchronous users with equal power and randomly generated spreading codes with spreading gain $G = 16$. The channel for each user had three fingers with considerable delay spread. The relative delays of the three multipath fingers were 1, 4, 9 chips for user 1 and 8, 12, 18 chips for user 2. The slot size was $M = 32$ and the same number of pilot symbols are included at the beginning of the slot of each user. This pilot symbols were used to remove the scaling ambiguity of the blind estimator. The signal-to-noise ratio (SNR) is defined by E_b/σ^2 where E_b is the bit energy and σ^2 is the chip noise variance (or the noise power spectrum density).

MSE and Cramér-Rao Bound We compared the proposed channel estimator using the decorrelating RAKE receiver (DRR) with the Cramér-Rao Bound and the conventional training based algorithm based on standard matched filter RAKE receiver (RR). For the training based RAKE receiver, pilot symbols were used to obtain the least squares channel estimate using the output of the (non-decorrelating) matched filter.

Fig. 5 shows the MSE performance for the case when a single pilot is used to remove the scaling factor. We observed that the conventional RAKE Receiver (RR) had a significant performance floor due to multiaccess interference. The Decorrelating RAKE Receiver (DRR), on the

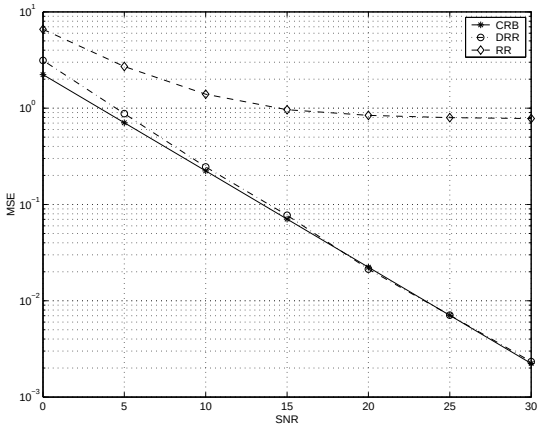

Figure 5: Channel MSE vs. SNR. Both users have three fingers with relative delays of 1, 4, 9 chips for user 1 and 8, 12, 18 for user 2. Five hundred Monte Carlo runs. One pilot symbol per user is used. Specific channel parameters are given in [12].

other hand, tracked CRB closely. We must note, however, that the gap of DRR to CRB increases as the number of user increases. This indicates that the proposed algorithm, while providing good channel estimate at high SNR, is not statistically efficient and may be improved using more sophisticated iterative schemes.

VI. Conclusion

In this paper, we considered the problem of channel estimation and symbol detection for long code CDMA. There are two main contributions. One is a new blind channel estimation and symbol detection algorithm. The technique can be easily amended for semiblind estimation, and it requires a small amount of samples. This makes the technique suitable for the rapid fading environment. The proposed approach uses the RAKE structure, which makes it possible to apply our algorithm to a subset of users in a group estimation setting.

The second contribution is an efficient implementation of the decorrelating matched filter using state-space techniques. This part is critical if the decorrelating RAKE is to be used in practice. Often there is a separate finger searcher in practical systems that identifies dominant multipaths, and finger locations and strength do vary. The proposed approach makes the implementation of decorrelating matched filter within implementation constraints.

There are further issues that go beyond the scope of this paper. For example, the the decorrelating process introduces coloring of the noise and bias in the estimator. Knowing the code matrix, we can remove such bias with additional processing. The proposed approach can be easily amended for multirate, multicode and multiantenna applications. Details can be found in [13].

References

[1] S. Verdú, *Multiuser Detection.* Cambridge, UK: Cambridge University Press, 1998.

[2] P. Dewilde and A. van der Veen, *Time-Varying Systems and Computations.* Dordrecht, The Netherlands: Kluwer Academic Publishers, 1998.

[3] Z. Yang and X. Wang, "Blind turbo multiuser detection for long-code multipath CDMA," *submitted to IEEE Trans. Signal Processing*, 2001.

[4] K. Li and H. Liu, "Channel estimation for DS-CDMA with aperiodic spreading codes," in *Proc. 1999 ICASSP*, pp. 2535–1538, Mar 1998.

[5] M. Torlak, B. Evans, and G. Xu, "Blind estimation of FIR channels in CDMA systems with aperiodic spreading sequences," in *Proc. 31st. Asilomar Conf. Sig. Systems and Computers*, (Montery, CA), pp. 495–499, Oct 1997.

[6] M. Zoltowski, Y. Chen, and J. Ramos, "Blind 2D RAKE receivers based on space-time adaptive MVDR processing for IS-95 CDMA system," in *Proceedings of the 15th IEEE MILCOM*, (Atlanta, GA), pp. 618–622, Oct 1996.

[7] N. Sidiropoulos and R. Bro, "User separation in DS-CDMA Systems with unknown Long PN Spreading Codes," in *Proc. IEEE-SPS Workshop on Signal Processing Advances in Wireless Communications (SPAWC99)*, (Annapolis, MD.), pp. 194–197, May 1999.

[8] Z. Xu and M. Tsatanis, "Blind channel estimation for long code multiuser CDMA systems," *IEEE Trans.Signal Processing*, vol. SP-48, pp. 988–1001, April 2000.

[9] C. Escudero, U. Mitra, and D. Slock, "A Toeplitz displacement method for blind multipath estimation for Long Code DS/CDMA signals," *IEEE Trans. Signal Processing*, vol. SP-48, pp. 654–665, March 2001.

[10] A. Weiss and B. Friedlander, "Channel estimation for DS-CDMA downlink with aperiodic spreading codes," *IEEE Trans.Communications*, vol. COM-47, pp. 1561–1569, Oct 1999.

[11] S. Buzzi and H. Poor, "Channel estimation and multiuser dection in long-code ds/cdma systems," *IEEE J. Select. Areas in Comm.*, vol. 19, pp. 1476–1487, August 2001.

[12] L. Tong, A. V. der Veen, P. Dewilde, and Y. Sung, "Blind decorrelating rake receiver for long code WCDMA," Tech. Rep. ACSP-02-01, Cornell University, Feb. 2002.

[13] L. Tong, A. V. der Veen, P. Dewilde, and Y. Sung, "Blind decorrelating rake receiver for long code WCDMA," *Submitted to IEEE Trans. Signal Processing*, Feb. 2002.